MULTI-ANTENNA INTERFERENCE COORDINATION IN DEVICE-TO-DEVICE ASSISTED HETEROGENEOUS CLOUD RADIO ACCESS NETWORKS

M. A. Abana*, R. Usman and K. L. Mathew

Department of Electrical and Electronics Engineering, Modibbo Adama University of Technology, Yola.

*****Corresponding Email Address: m.a.abana@mautech.edu.ng

ABSTRACT

In this paper, a stochastic geometry based framework is developed to investigate the performance of multi-antenna interference coordination utilizing two remote radio head (RRH) cooperation schemes namely, zero force beamforming (ZFBF) and non-coherent joint coordinated transmission (NC-JCT). Studies have shown that despite the benefit offered by RRH cooperation in improving the performance of some selected down link users, this gain actually comes at the cost of disabling other downlink users from being served on the same channels and thus leading to inefficient spectral resource utilization. To address this problem, Device-to-Device (D2D) communication is utilized to serve as an alternative for users, which has shown to be effective in improving the spectral utilization. Results from the analysis indicates that enabling D2D communication can effectively offload the heterogeneous cloud radio access network (H-CRAN) and provide significant benefits in terms of improved spectral utilization. The results also show that the area spectral efficiency (ASE) of D2D users when ZFBF scheme is applied performs better than that of NC-JCT counterpart.

Keywords: Heterogeneous cloud radio access networks, interference coordination, Coverage Probability and Area Spectral Efficiency.

1 INTRODUCTION

Data traffic in wireless communication networks has been increasing exponentially over the past decade and this trend is expected to continue [1]. The emergence of data-hungry applications, such as video-on-demand and online gaming as well as the exploding number of smart mobile devices demands the introduction of aggressive technologies. To facilitate these needs, the fifth generation (5G) network is envisioned to achieve 1000X capacity enhancement and save up to 90% of the network energy consumption compared with the fourth generation (4G) networks [2]. Heterogeneous cloud radio access network (H-CRAN) has been recognized as one of the key enabler for the 5G network [3]. H-CRANs integrate the cloud computing technology into heterogeneous networks (HetNets) to realize a large scale cooperative signal processing and networking functionalities with a cost effective potential of achieving substantial performance improvement compared to the existing HetNets [3, 4]. It consists of high power nodes (HPNs) e.g., macro/micro base stations (MBS) and low power nodes (LPNs) e.g., Picocells, femtocells, remote radio heads (RRHs), linked to a centralized baseband unit (BBU) via the backhaul and fronthaul, respectively. The incorporation of HPNs is critical to guarantee the 5G requirement of backward compatibility with the traditional MBS system and provide support for seamless coverage, while the LPNs are used to provide high-speed data transmission in the hot spots with huge data requirements.

The RRHs in H-CRAN are capable of aggressively reusing the existing spectrum to support high data rate applications. However, spectrum reuse in H-CRAN causes strong interference, especially when the RRHs are densely deployed. This affects the achievable signal-to-interference-plus-noise-ratio (SINR) at each user and hence a major limiting factor of wireless network performance. Fortunately, unlike the traditional HetNets, interference among dense RRHs in H-CRANs can be alleviated through large-scale centralized cooperative processing at the BBU pool. Generally,

cooperative processing techniques in H-CRAN system may range from coordinated beamforming (CB) to joint cooperative transmission (JCT) [5].

Coordinated beamforming has been reported to deliver significant performance gains in terms of coverage probability, spectral and energy efficiency [6, 7]. For example, an optimal coordinated beam former design problem was formulated for a multi-cell downlink network in [6], which shows that, under the same SINR targets, a carefully designed coordinated beamforming scheme is capable of significantly reducing the transmit power as compared to the conventional non-cooperative approach. To achieve an effective beamformer design, it is necessary for the RRHs to have a full knowledge of channel state information (CSI) condition of all users. However, acquiring perfect CSI is limited by bandwidth and delay-limited fronthaul in practice. Hence, the performance of CB scheme is limited by the accuracy of CSI estimation. On the contrary, non-coherent JCT (NC-JCT) does not require the availability of perfect CSI. In NC-JCT scheme, multiple copies of the same data is sent from all the cooperating RRHs to the served user in the downlink without any prior phase mismatch correction or tight synchronization [8]. It is reported that in some cases, NC-JCT outperforms its coherent counterpart due to less stringent synchronization and CSI requirements [9]. Lee in [8], developed a tractable model to analyze the performance benefits of NC-JCT of generic downlink users.

Despite benefits of mitigating inter-cell interference, RRH cooperation through clustering may not be a suitable scheme for a heavily-loaded network, because depending on the coordination strategy, only a limited number of users can be simultaneously served within a given cluster and thus leading to waste of spectral resource. In other words, RRH coordination is beneficial to only some selected users, for example users at the cell-edge and this may lead to potential spectral efficiency degradation from the system perspective, especially when the network is heavily loaded. To this effect, this paper considers the integration of D2D communication in H-CRAN with the aim of improving the spectral utilization of the entire network. D2D communications enables the establishment of direct communication link between users without unnecessary routing of traffic through the cellular network infrastructure, resulting in shorter transmission distances and improved data rates [10].

D2D communications was standardized by the 3rd Generation Partnership Project (3GPP) presented in LTE Release 12, in parallel to the standardization efforts, D2D communications have been actively studied by the research community. For example, the authors in [11], proposed a D2D underlaid HetNets operating with dynamic time-division duplex, where the D2D transmitters follow a carrier sensing multiple access scheme to protect the ongoing cellular and D2D transmissions. An analytical framework to evaluate the load-aware coverage probability and network throughput is presented in [11]. In [12], two cellular tiers operating in disjoint bands while the D2D tier utilizes both bands is considered, where the optimal D2D link density and transmit power that maximizes the achievable transmission capacity are derived. H-CRAN with non-uniformly D2D deployment is considered in [13], performance in terms of average data delivery latency in a fronthaul constrained H-CRAN was analyzed, where it was shown that the non-uniform D2D deployment achieves a lower average traffic delivery latency compared with the uniform D2D deployment and the pure H-CRAN deployment scenarios. A cooperative interference cancelation in the downlink cellular system using D2D to improve the performance of interference cancelation by enabling nearby users to share information regarding correlated interference was studied in [14]. Meanwhile, a strategy based on coordination and zero forcing algorithm is identified to eliminate interference between D2D and cellular system, thereby boosting the overall system throughput [15].

Despite the fact that incorporating D2D communications have shown to effectively improve spectral efficiency of the overall network, the best RRH coordination scheme to be adopted when D2D communications is underlaid in H-CRAN is yet to be determined, which motivates our work. We investigate the benefits of incorporating D2D communication on improving the area spectral efficiency (ASE) of H-CRAN for the two RRH coordination schemes. The main contributions of this paper are summarized as follows:

- D2D assisted multi-antenna H-CRAN system model is developed to characterize the performance of a typical user in the downlink scenario for two coordination schemes namely, ZFBF and NC-JCT. The model also considered a hybrid system where users can select to be

served by cooperative RRHs or D2D transmitters (DTs) according to distance based mode selection criteria.

- A framework to derive the approximate SIR coverage for both ZFBF and NC-JCT was developed utilizing tools from stochastic geometry.
- Results from the analysis indicates that enabling D2D communication can effectively offload the H-CRANs and provide significant benefits in terms of improved spectral utilization

The rest of this paper is organized as follows. Section 2 presents the system description and proposed the approach, Section 3 provide the analysis of SIR distribution and evaluate the downlink ASE for the cellular and D2D users under both ZFBF and NC-JCT schemes. Simulation results are discussed in Section 4 and conclusions are drawn in Section 5.

2 SYSTEM MODEL

The model under study is a hybrid network consisting of both cellular network and D2D communication links. For the cellular network, we consider H-CRAN architecture with the HPNs and RRHs linked to a centralized BBU pool via the backhaul and fronthaul respectively. The location of HPNs and RRHs are modeled on two-dimensional plane $\mathbb{R}^2$ according to homogeneous Poisson point process (PPP), Φ_1 and Φ_2 with densities λ_1 and λ_2 respectively. Each HPN is equipped with N_1 transmit antennas with total transmit power P_1 and RRHs are equipped with N_2 antennas with total transmit power P_2. Single antenna users are distributed on $\mathbb{R}^2$ according to homogeneous PPP Φ_u of density λ_u. D2D transmitters (DTs) are selected from users with adequate storage and processing capabilities and are located within short distances to their target receivers. Assume a fraction η of users met the required condition for D2D communication and are considered as the potential DTs. The location of the DTs can therefore be modeled by independent thinning of the PPP Φ_u with probability η, i.e., the set of potential DTs forms PPP Φ_3 with density $\lambda_3 = \eta\lambda_u$. Similar to the system model in [11], we assume that each potential DTs has an assigned receiver (not members of Φ_u) with fixed transmit power P_3.

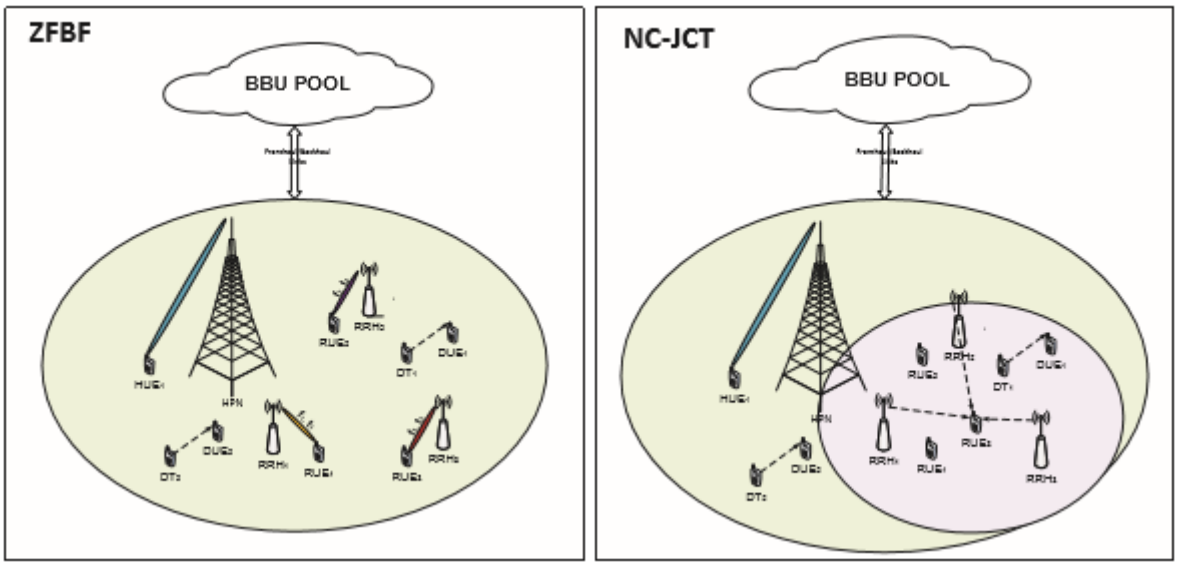

Figure 1. Illustration of the system model describing the two cooperative interference coordination schemes Viz: ZFBF and NC-JCT.

2.1 Transmission schemes

The analysis in this paper considered a typical user U_0 located at the origin, this is assumption is allowed by Slivnyaks theorem [8], which states that the properties observed by a typical point of a PPP is same as those observed by a node at origin in the process. Since the HPN is used to mainly deliver the control signaling and guarantee the basic coverage for large area, only users requiring services with low traffic arrival rates are assumed to be served by HPN, while users requiring high bit

rate services are jointly served by multiple RRHs in a user-centric fashion or by a potential DT. Our analysis will mainly focus on RRH and D2D served users.

We now describe the cooperative IC scheme utilize by the transmitters to mitigate the network interference. For the HPN, inter-tier IC is employed to avoid interference to RRH served users receiving strong interference by making use of at most U ($U < N_1$) DoF at each HPN, while interference to the rest of the users is avoided by employing coordinated scheduling. In particular, low-complexity ZFBF precoder is utilized at each HPN to perform inter-tier IC, while the remaining $N_1 - U$ antennas at the HPN are used for boosting the signal to its scheduled user. Specifically, denote $\mathbf{H_{1,0}} = [h_{1,0}, g_{1,1}, ..., g_{1,U}]^{\dagger}$, where $h_{1,0} \sim CN(0_{N1\times 1}, I_{N1})$ represents the channel vector between HPN and its scheduled user, and $g_{1,i} \sim CN(0_{N1\times 1}, I_{N1})$ denotes the channel vector between HPN and the RRHs receiving the i^{th} strongest interference ($i = 1,2,....U$). The ZFBF precoding matrix at the HPN is designed as $\mathbf{W_{1,0}} = \mathbf{H^{\dagger}_{1,0}(H_{1,0}H^{\dagger}_{1,0})^{-1}}$ and the ZFBF vector at HPN is designed as $f_{1,0} = w_{1,0} / \|w_{1,0}\|$ where $w_{1,0}$, is a vector representing the first column of the matrix $\mathbf{W_{1,0}}$. The corresponding SIR at the U_0 when served by the HPN is written as:

$$SIR_{1,BF} = \frac{P_1 \left| h_{i,00} f_{1,00} \right|^2 r_{i,00}^{-\alpha}}{\tilde{I}_1 + I_2 + I_3} \tag{1}$$

Where

$$\tilde{I}_1 = \sum_{j\in\Phi_1/\{0\}} P_1 \left\| h_{1,j0} f_{1,j0} \right\|^2 r_{1,j0}^{-\alpha}, \quad I_2 = \sum_{j\in\Phi_2} P_2 \left\| h_{2,j0} f_{2,j0} \right\|^2 r_{2,j0}^{-\alpha}, \quad I_3 = \sum_{j\in\Phi_3} P_3 \left\| h_{2,j0} \right\|^2 r_{3,j0}^{-\alpha}$$

For the RRH transmission, we leverage the centralized processing capabilities in C-RAN and consider a user centric coordination policy. In particular, each RRH joins a cooperating cluster C_0 if it is located within a ball of radius r_c centered at the origin (0, 0) $\in R_2$ denoted by $\mathcal{B}(0, r_c)$. Here, the size of the cooperative cluster can either be determined using the number of cooperating RRHs or cooperative cluster radius. In this paper, we adopt the cluster radius r_c to define the cluster size, since (for a given RRH density λ_2) the number of cooperating RRHs can be control by the cluster radius. We consider two cooperative transmission scheme within each cluster namely (1) ZFBF (2) NC-JCT.

1.) ZFBF: In this case, the typical user U_0 is associated with the nearest RRH_0 in C_0, and the other ($min(N_2, |C_0|) - 1$) RRHs in C_0 are chosen to cooperatively serve the other users in C_0. Here, $|.|$ denotes the cardinality operation, accordingly, each RRH uses $|C_0| - 1$ antennas for interference cancelation and the remaining $N_2 - |C_0| + 1$ antennas are used for boosting the signal of the scheduled user. Meanwhile, if the number of RRHs in C_0 is greater than N_2, only N_2 RRHs can be active on the utilized resource block by U_0 while the remaining RRHs cooperate by not transmitting. The ZFBF precoder at each RRH can be obtained in a similar fashion as that of the HPN, which can be written as $\mathbf{W_{2,0}} = \mathbf{H^{\dagger}_{2,0}(H_{2,0}H^{\dagger}_{2,0})^{-1}}$. The ZFBF vector at HPN is designed as $f_{2,0} = w_{2,0} / \|w_{2,0}\|$ where $w_{2,0}$, is a vector representing the first column of the matrix $\mathbf{W_{2,0}}$. The corresponding SIR at the U_0 in this case is written as follows:

$$SIR_{2,BF} = \frac{P_2 \left\| h_{2,00} f_{2,00} \right\|^2 r_{2,00}^{-\alpha}}{I_1 + \tilde{I}_{2,BF} + I_3} \tag{2}$$

Where $I_1 = \sum_{j\in\Phi_1} P_1 \left\| h_{1,j0} \right\|^2 r_{1,j0}^{-\alpha}$, $\tilde{I}_{2,BF} = \sum_{j\in\Phi_2\setminus C_0} P_2 \left\| h_{2,j0} f_{2,j0} \right\|^2 r_{2,j0}^{-\alpha}$ and I_3 is defined in (1)

2.) NC-JCT: In this case, all the RRHs in C_0 cooperate to serve U_0 by jointly transmitting copies of the same data to U_0 thereby turning interference from all the RRHs in the C_0 to useful signals. In this work, we consider NC-JCT where copies of the same data is transmitted by each RRH without any prior phase matching and tight synchronization [8]. The sum of the received non-coherent signals results in boosting the received signal power at the user. NC-JCT surpasses the coherent counterpart in some case due to less stringent synchronization and CSI requirements [16].

$$SIR_{2,JT} = \frac{\left\| \sum_{i \in C_0} \sum_{m=1}^{N_2} \sqrt{P_{2,m}} h_{2,i0} r_{2,i0}^{-\alpha} \right\|^2}{I_1 + \tilde{I}_{2,JT} + I_3} \tag{3}$$

Where I_3 and I_1 are defined in (1) and (2) respectively, and $\tilde{I}_{2,JT} = \left\| \sum_{j \in \Phi_2 \setminus C_0} \sum_{m=1}^{N_2} \sqrt{\bar{P}_2} h_{2,j0} r_{2,j0}^{-\alpha} \right\|^2$

To enable the D2D communications, distance based mode selection is considered, in particular D2D mode is activated only when the distance between the reference *UE* and the potential *DT*, is less than a specified threshold r_{th}. In this case, the achievable SIR at the D2D receiving *UE* is given as:

$$SIR_3 = \frac{P_3 \left\| h_{3,00} \right\|^2 r_{3,00}^{-\alpha}}{I_1 + I_2 + I_3} \tag{4}$$

Where $I_2 = I_{2,BF} = \sum_{j \in \Phi_2} P_2 \left\| h_{2,j0} f_{2,j0} \right\|^2 r_{2,j0}^{-\alpha}$ when ZFBF scheme is employed by the RRHs and

$I_2 = I_{2,JT} = \left\| \sum_{j \in \Phi_2} \sum_{m=1}^{N_2} \sqrt{P_{2,m}} h_{2,j0} r_{2,j0_m}^{-\alpha} \right\|^2$, when NC-JCT scheme is employed by the RRHs. I_3 and I_1 are defined in (1) and (2) respectively. Meanwhile, we assume that the distance to the serving DT, $r_{3,00}$ follows Rayleigh distribution with PDF given as

$$f_{r_D(x)} = 2\pi exp(-\pi x^2) \tag{5}$$

2.2 Performance metric

To study the performance of the described model, we consider interference limited scenario and ignore the thermal noise since the system interference is dominant. Analysis with thermal noise can be performed in a similar fashion. We first derive the achievable SIR coverage at a typical user when served by both the cellular and D2D network respectively. Then based on the derived SIR coverage expression, we obtain the ASE of the system which is the main performance metric used in this paper. The ASE is defined as the achievable data rate per unit area; it is aimed at characterizing the benefits of D2D communication on improving the performance of the H-CRAN system. Additionally, the ASE is utilized to compare the effect of D2D communication on the two cooperative transmission schemes adopted. The ASE when ZFBF cooperation scheme is utilized is given as:

$$\mathrm{A}_{BF} = \lambda_1 \mathrm{E}\left[R_{1,BF} \right] + \frac{\mathrm{E}\left[R_{2,BF} \right]}{\pi r_c^2} + \lambda_3 \mathrm{E}\left[R_{3,BF} \right] \tag{6}$$

Similar ASE expression can be obtained when NC-JCT is employed, which is written as

$$\mathrm{A}_{JT} = \lambda_1 \mathrm{E}\left[R_{1,JT} \right] + \frac{\mathrm{E}\left[R_{2,JT} \right]}{\pi r_c^2} + \lambda_3 \mathrm{E}\left[R_{3,JT} \right] \tag{7}$$

3 PERFORMANCE ANALYSIS OF COOPERATIVE TRANSMISSION SCHEMES

In this section, we analyze system performance under the two described RRH cooperation schemes. From the expressions of the SIR for the RRH and D2D users, we see that the interference experienced by the RRHs can be eliminated at the expense of sacrificing the spatial degrees of freedom for the served users. Therefore, the effects of the cooperative schemes employed at the RRHs on system performance is the focus of the following paragraphs, i.e., we characterize the SIR coverage probability and ASE when the RRHs uses the different cooperative interference coordination schemes.

3.1 Zero force beamforming (ZFBF)

In the following, first we study the SIR coverage probability when ZFBF scheme is applied at the RRHs. For the HPN served reference UE, the SIR coverage is obtained as follows:

$$\mathrm{P}(SIR_1^{BF} \geq T) = \mathrm{P}\left[\left\| h_{1,0} f_{1,00} \right\|^2 \geq \frac{T}{P_1 r_{1,00}^{-\varepsilon}} I_{1,eff} \right], \qquad \overset{(a)}{=} E_{s_1}\left[\sum_{i=0}^{N_1-U} \frac{(s_1)^i}{\Gamma(i)} \mathcal{L}_{I_{1,eff}}^{(i)}(s_1) \right] \tag{8}$$

Where $I_{1,eff} = I_1 + I_{2,BF} + I_3$, $s_1 = \frac{T}{P_1 r_{1,00}^{-\alpha}}$ and (a) follows from the fact that $\left\| h_{1,0} f_{1,00} \right\|^2 \sim \Gamma((N_1 - U),1)$

$$\text{In (8)}, \mathcal{L}_{I_{1,eff}}(s_1) = \mathcal{L}_{\tilde{I}_1}(s_1)\mathcal{L}_{I_{2,BF}}(s_1)\mathcal{L}_{I_3}(s_1), \tag{9}$$

Where we have;

$$\mathcal{L}_{\tilde{I}_1}(s_1) \overset{(a)}{=} exp(-2\pi\lambda_1 \int_{r_{1,00}}^{\infty} r(1 - \frac{1}{1+s_1 P_1 r^{-\alpha}})dr)$$

$$= exp(-\pi\lambda_1 \frac{s_1 P_1 r^{2-\alpha}}{\alpha - 2} Z_\alpha(s_1 P_1 r^{-\alpha})) \tag{10}$$

Where (a) follows from probability generating functional (PGFL) of PPP, and

$Z_a(b) = {}_2F_1(1, 1-\frac{2}{\alpha}, 2-\frac{2}{\alpha}, -b)$

$$\mathcal{L}_{I_{2,BF}}(s_1) = exp(-2\pi\lambda_2 \int_0^{\infty} r(1 - \frac{1}{1+s_1 P_2 r^{-\alpha}})dr)$$

$$= exp\left[-(s_1 P_2)^{\frac{2}{\alpha}} \frac{2\pi^2 \lambda_2}{\alpha sin(\frac{2\pi}{\alpha})} \right] \tag{11}$$

$\mathcal{L}_{I_3}(s_1)$ is similarly evaluated as:

$$\mathcal{L}_{I_3}(s_1) = exp\left[-(s_1 P_3)^{\frac{2}{\alpha}} \frac{2\pi^2 \lambda_3}{\alpha sin(\frac{2\pi}{\alpha})} \right] \tag{12}$$

Therefore, by combining (10), (11) and (12), $\mathcal{L}_{I_{1,eff}}(s_1)$ in (9) can be obtain. Accordingly, we derive the SIR coverage in (8).

For the RRH served *UE*, the *SIR* coverage is similarly obtaining as:

$$P\left[SIR_{2,BF} \geq T \right] = \mathrm{E}_{s_2}\left[\sum_{i=0}^{N_2 - |C_0|} \frac{(s_2)^i}{\Gamma(i)} \mathcal{L}_{I_{2,eff}}^{(i)}(s_2) \right] \tag{13}$$

Where $I_{2,eff} = I_1 + \tilde{I}_{2,BF} + I_3$ and $s_2 = \frac{T}{P_2 r_{2,00}^{-\alpha}}$.

The Laplace transform in (13) is evaluated as follows

$$\mathcal{L}_{I_{2,eff}}(s_2) = \mathcal{L}_{I_1}(s_2)\mathcal{L}_{\tilde{I}_{2,BF}}(s_2)\mathcal{L}_{I_3}(s_2)$$

Where

$$\mathcal{L}_{I_1}(s_2) = exp\left[-(s_2 P_1)^{\frac{2}{\alpha}} (\frac{2\pi^2 \lambda_1}{\alpha sin(\frac{2\pi}{\alpha})}) \right], \tag{14}$$

$$\mathcal{L}_{\tilde{I}_{2,BF}}(s_2) = exp\left[-\pi\lambda_2 \frac{s_2 P_2 r^{2-\alpha}}{\alpha - 2} Z_\alpha(s_2 P_2 r^{-\alpha}) \right], \tag{15}$$

$$\mathsf{L}_{I_3}(s_2) = exp\left[-(s_2P_3)^{\frac{2}{\alpha}}\left(\frac{2\pi^2\lambda_3}{\alpha sin(\frac{2\pi}{\alpha})}\right)\right] \tag{16}$$

By combining (14), (15) and (16), $\mathsf{L}_{I_{2,eff}}(s_2)$ can be evaluated. Accordingly, the solution to SIR coverage in this case can be obtained.

For U_0 selected to be served by *DT*, the SIR coverage is evaluated as follows:

$$P\left[SIR_{3,BF} \geq T\right] = P\left[\left\|h_{3,00}\right\|^2 \geq \frac{T}{P_3 r_{3,00}^{-\alpha}} I_{3,eff}\right]$$
$$\overset{(a)}{=} E_{r_{3,00}}\left[\mathsf{L}_{I_1}(s_3)\mathsf{L}_{I_{2,BF}}(s_3)\mathsf{L}_{\tilde{I}_3}(s_3)\right] \tag{17}$$

Where (a) follows from the fact that $\left\|h_{3,00}\right\|^2 \sim exp(1)$ and $s_3 = \frac{T}{P_3 r_{3,00}^{-\alpha}}$. The Laplace transforms of I_1, $I_{2,BF}$ and I_3 evaluated at s_3 similar to (14), (11) and (12), given respectively as follows:

$$\mathsf{L}_{I_1}(s_3) = exp\left[-(s_3P_1)^{\frac{2}{\alpha}}\left(\frac{2\pi^2\lambda_1}{\alpha sin(\frac{2\pi}{\alpha})}\right)\right], \tag{18}$$

$$\mathsf{L}_{I_{2,BF}}(s_3) = exp\left[-(s_3P_2)^{\frac{2}{\alpha}}\left(\frac{2\pi^2\lambda_2}{\alpha sin(\frac{2\pi}{\alpha})}\right)\right], \tag{19}$$

$$\mathsf{L}_{\tilde{I}_3}(s_3) = exp\left[-(s_3P_3)^{\frac{2}{\alpha}}\left(\frac{2\pi^2\lambda_3}{\alpha sin(\frac{2\pi}{\alpha})}\right)\right] \tag{20}$$

Note that in (17) the expectation with respect to $r_{3,00}$ applies since U_0 only select *DT* based on the condition that $r_{3,00} \leq r_{th}$, thus the conditional PDF of $r_{3,00}$ is given as

$$f_{r_{3,00}|r_{3,00}\leq r_{th}}(x) = \frac{2\pi x exp(-\pi x^2)}{1-exp(-\pi r_{th}^2)} \tag{21}$$

By substituting (18), (19) and (20) into (17) and marginalizing the expectation with the PDF of $r_{3,00}$ in (21), we obtain the SIR coverage as

$$P\left[SIR_{3,BF} \geq T\right] = \frac{1-exp\left[\pi r_{th}^2\left\{1+\lambda'_{3,BF}\right\}\right]}{\left\{1+\lambda'_{3,BF}\right\}(1-exp(-\pi r_{th}^2))} \tag{22}$$

Where $\lambda'_{3,BF} = \frac{2\pi T^{\frac{2}{\alpha}}}{\alpha sin(\frac{2\pi}{\alpha})}\left(\left(\frac{P_1}{P_3}\right)^{\frac{2}{\alpha}}\lambda_1 + \left(\frac{P_2}{P_3}\right)^{\frac{2}{\alpha}}\lambda_2 + \lambda_3\right)$

Next, we evaluate the ASE, to demonstrate the benefit integrating D2D communication in existing H-CRAN system. To determine the ASE given in (6), we first evaluate the expectation of the achievable data rate E[R] at U_0 when served by *HPN*, *RRH* and *DT*, respectively. E[R] can be obtained according to the derivation in [9] given as

$$\mathrm{E}\left[R\right] = \int_0^\infty log(1+T)\, f_{SIR}(T)dT = \int_0^\infty \frac{log_2 e}{(1+T)} F_{SIR}(T)dT \tag{23}$$

Where $F_{SIR}(T)$ is the CCDF of the *SIR*. Accordingly, by substituting the expressions for the *SIR* coverage (which is equivalently the CCDF of the SIR) given in (8), (13) and (22) for U_0 served by *HPN*, *RRHs* or *DT* respectively, into (23), we arrive at the achievable data rate. Finally, the ASE is obtained according to the expression in (6).

3.2. Non-coherent joint coordinated transmission (NC-JCT)

When the NC-JCT scheme is adopted, the *SIR* at U_0 when served by the *HPN* given in (1) can be re-written as:

$$SIR_{1,JT} = \frac{P_1 \left\| h_{1,0} f_{1,00} \right\|^2 r_{1,00}^{-\alpha}}{\tilde{I}_1 + I_{2,JT} + I_3} \tag{24}$$

Accordingly the *SIR* coverage is given in (8), the difference being the Laplace transform of $I_{2,JT}$, is evaluated as follows:

$$\begin{aligned} \mathsf{L}_{I_{2,JT}}(s_1) &= \mathrm{E}_{\Phi_2}\left[exp(-s_1 G_{2,i0} \tilde{P}_2 r_{2,j0}^{-\alpha}) \right] \\ &\overset{(a)}{=} \mathrm{E}_{\Phi_2}\left[\prod_{j \in \Phi_2} \frac{1}{1+exp(-s_1 \tilde{P}_2 r_{2,j0}^{-\alpha})^{N_2}} \right] \\ &\overset{(b)}{=} exp\left[-2\pi\lambda_1 \int_0^{\infty} r\left(1 - \frac{1}{1+exp(-s_1 \tilde{P}_2 r^{-\alpha})^{N_2}} dr \right] \right. \\ &\overset{(c)}{=} exp\left[-(s_1 \tilde{P}_2)^{\frac{2}{\alpha}} \frac{2\pi^2 \lambda_2}{\alpha sin(\frac{2\pi}{\alpha})} \prod_{i=2}^{N_2} \left(\frac{2}{\alpha(i-1)} + 1\right) \right] \end{aligned} \tag{25}$$

Where $G_{2,i0} = \sum_{m=1}^{N_2} \left\| h_{2,i0_m} \right\|^2$, (a) follows because $G_{2,i0} \sim \Gamma(N_2, 1)$, (b) follows from the PGFL of PPP and (c) follows from the derivation of equation (30) in [17]. Accordingly, we derive the SIR coverage according to (8).

For U_0 selected to be served by *DT*, the achievable *SIR* is given in (1), which can be re-written as:

$$SIR_{3,JT} = \frac{P_3 \left\| h_{3,00} \right\|^2 r_{3,00}^{-\alpha}}{I_1 + I_{2,JT} + \tilde{I}_3} \tag{26}$$

The SIR coverage is evaluated using similar steps as that of the ZFBF case and is written as follows:

$$P\left[SIR_{3,JT} \geq T \right] = E_{r_{3,00}}\left[\mathsf{L}_{I_1}(s_3) \mathsf{L}_{I_{2,JT}}(s_3) \mathsf{L}_{\tilde{I}_3}(s_3) \right] \tag{27}$$

Where $\mathsf{L}_{I_1}(s_3)$, $\mathsf{L}_{I_{2,JT}}(s_3)$ and $\mathsf{L}_{\tilde{I}_3}(s_3)$ are respectively obtained based on (18), (25), (20). Therefore, by marginalizing the expectation in (27) with the PDF of $r_{3,00}$, we obtain the SIR coverage as:

$$P\left[SIR_{3,JT} \geq T \right] = \frac{1 - exp\left[\pi r_{th}^2 \left\{ 1 + \lambda'_{3,JT} \right\} \right]}{\left\{ 1 + \lambda'_{3,JT} \right\} (1 - exp(-\pi r_{th}^2))} \tag{28}$$

Where $\lambda'_{3,JT} = \frac{2\pi T^{\frac{2}{\alpha}}}{\alpha sin(\frac{2\pi}{\alpha})} \left(\left(\frac{P_1}{P_3}\right)^{\frac{2}{\alpha}} \lambda_1 + \left(\frac{\tilde{P}_2}{N_2 P_3}\right)^{\frac{2}{\alpha}} \prod_{i=2}^{N_2} \frac{2}{\alpha(i-1)} + 1 \right) \lambda_2 + \lambda_3 \right)$

To evaluate the ASE for the NC-JCT case, we first calculate E[R] by directly substituting the CCDF of the *SIR* obtained in (8), (13) and (28) when U_0 is served by *HPN*, *RRHs* or *DT* respectively, into (23). Finally, the ASE is obtained according to (7).

3.3 Analytic comparison of the two RRH coordination schemes

In this section, we provide an analytic comparative study to establish the RRH cooperation scheme that is more suitable for *D2D* users. We observe from (23) that comparing the achieved ASE by *D2D* transmission when ZFBF and NC-JCT scheme is employed is equivalent to comparing $F_{SIR_{3,BF}}(T)$ with $F_{SIR_{3,JT}}(T)$. Notice from (22) and (28) that $F_{SIR_{3,BF}}(T)$ and $F_{SIR_{3,JT}}(T)$ are in similar form. Therefore it is easy to show that if for example $\lambda_{3,JT}^{'} > \lambda_{3,BF}^{'}$, then using ZFBF offers higher *D2D* performance and vice versa. To achieve such goal, we compute the difference of $\lambda_{3,JT}^{'}$ and $\lambda_{3,BF}^{'}$ i.e

$$\lambda_{3,JT}^{'} - \lambda_{3,BF}^{'} = \frac{2\pi T^{\frac{2}{\alpha}} \lambda_2}{\alpha \sin(\frac{2\pi}{\alpha})} \left[N_2^{-\frac{2}{\alpha}} \prod_{i=2}^{N_2} (\frac{2}{\alpha(i-1)} + 1) - 1 \right] \tag{29}$$

Obviously, in (29) if $W(N_2) = N_2^{-\frac{2}{\alpha}} \prod_{i=2}^{N_2} (\frac{2}{\alpha(i-1)} + 1) > 1$, a better ASE can be achieved by the coexistence of D2D with ZFBF enabled H-CRANs than the NC-JCT counterpart. Note that $W(N_2)$ is an increasing function of N_2 since $\tilde{W}(N_2) = \frac{W(N_2+1)}{W(N_2)} = \frac{N_2^{\frac{2}{\alpha}}(N_2+\frac{2}{\alpha})}{(N_2+1)^{\frac{2}{\alpha}} N_2} > 1$ which can be proved by showing that $\frac{d\tilde{W}(N_2)}{dN_2} > 0$ and $\tilde{W}(1) > 1$ therefore, we prove $\tilde{W}(2) > 1$ since $N_2 \geq 1$, hence by re-writing $\tilde{W}(2) = \frac{\tilde{W}_2(\frac{2}{\alpha})}{\tilde{W}_3(\frac{2}{\alpha})}$, where $\tilde{W}_2(\frac{2}{\alpha}) = \frac{2}{\alpha} + 1$ and $\tilde{W}_3(\frac{2}{\alpha}) = 2^{\frac{2}{\alpha}}$ for all $0 < \frac{2}{\alpha} < 1$.

When $\frac{2}{\alpha} \to 0$, $\tilde{W}_2(\frac{2}{\alpha}) \to 1$ and $\tilde{W}_3(\frac{2}{\alpha}) \to 1$, and when $\frac{2}{\alpha} \to 1$, $\tilde{W}_2(\frac{2}{\alpha}) \to 2$ and $\tilde{W}_3(\frac{2}{\alpha}) \to 2$ $\tilde{W}_2(\frac{2}{\alpha}) > \tilde{W}_3(\frac{2}{\alpha})$. Meanwhile it can also be shown that $\tilde{W}_3(\frac{2}{\alpha})$ is a convex function of $\frac{2}{\alpha}$ and $\tilde{W}_2(\frac{2}{\alpha})$ is a linear function of $\frac{2}{\alpha}$, hence $\tilde{W}_2(\frac{2}{\alpha}) > \tilde{W}_3(\frac{2}{\alpha})$ for all $0 < \frac{2}{\alpha} < 1$, therefore $\tilde{W}(2)$, consequently $\lambda_{3,JT}^{'} > \lambda_{3,BF}^{'}$.

From the above analysis it follows that the *ASE* achieved by *D2D* UEs when ZFBF is adopted outperforms that achieved with NC-JCT scheme. Intuitively this can be explaining from the fact that when ZFBF is applied the channel is normalized by the beamforming vector before transmission and the effective normalized channel gain is lower than that of the NC-JCT.

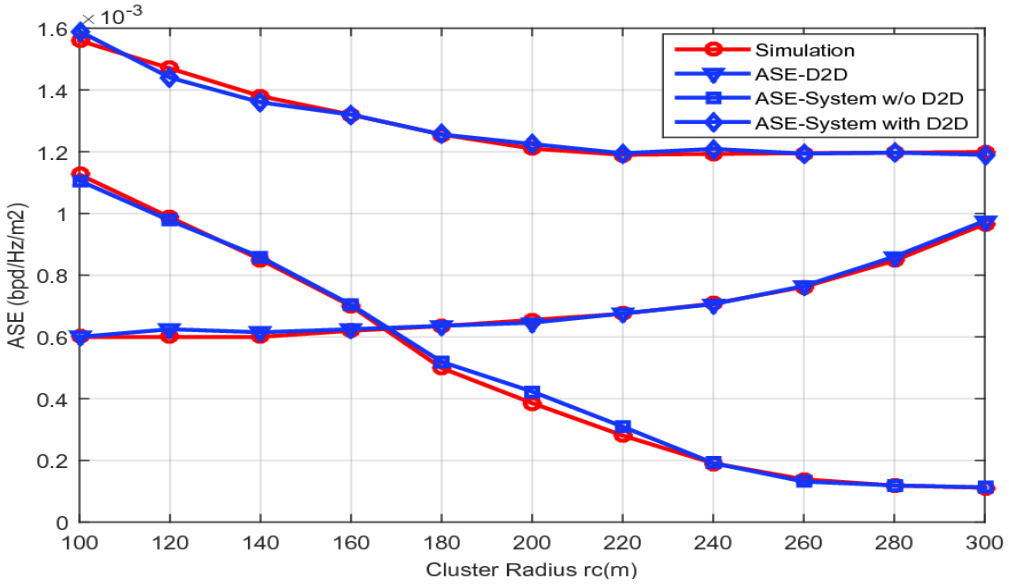

Figure 2. ASE with varying cluster radius r_c under ZFBF scheme

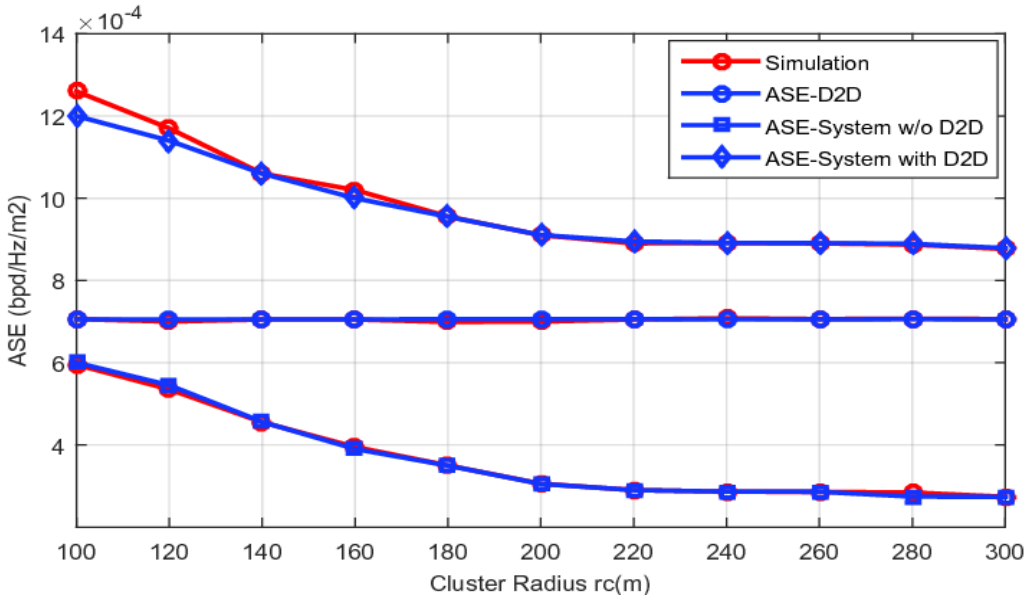

Figure 3. ASE with varying cluster radius r_c under NC-JCT scheme

Accordingly, RRHs interference to *D2D* UEs is reduced when ZFBF is adopted and thus achieving a higher ASE.

4 RESULTS AND DISCUSSION

In this section the performance of the two considered multi-antenna IC schemes in *D2D* assisted H-CRAN were evaluated. Some important aspects of the simulation setup are described as follows: The location of the *HPNs*, *RRHs* and *DTs* are realized as homogeneous PPPs in an area of $1000\times1000m^2$ with densities $\lambda_1 = \frac{1}{\pi 500^2}$, $\lambda_2 = \frac{6}{\pi 500^2}$ and $\lambda_3 = \frac{12}{\pi 500^2}$, respectively. Using MATLAB based Monte Carlo simulation method, an experiment with *10,000* independent channel state realization were conducted from which the average is taken. In each realization, a downlink *UE* select to be served by either *RRHs* or a potential *DT* based on the distance based selection criteria described in section 2. It is worthy of note here that *HPN* is dedicated to serve *UEs* with low bit rate requirement. It was also assumed that the *HPNs* are always active. The curves obtained from the simulations are compared with the analytical results to verify its effectiveness. Default simulation parameters are set as follows: $\alpha = 4$, $P_1 = 43dBm$, $P_2 = 33dBm$, $P_3 = 23dBm$, $N_1 = 8$, $N_2 = 6$ [18]. Figures 2 and 3 plots the ASE as a function of RRH cluster radius r_c when ZFBF and NC-JCT are utilized by the *RRHs* respectively.

It can be observed from Figure 2 that the ASE decreases with increasing r_c, this is because as r_c is increased, the number of RRHs in the cooperation cluster increases, which means that more RRHs needs to cooperate through coordinated scheduling and thus remain inactive on the resource blocks utilized by U_0. Similarly, Figure 3 shows that the ASE decreases with increasing r_c, this is because increasing r_c means more RRHs will jointly serve U_0, however useful signal received from far away RRHs is usually negligible, meanwhile only a small number of users can be simultaneously served leading to inefficient spectral resource utilization. Consequently, by enabling D2D communications, more users can be active simultaneously on each channel leading to improve ASE performance. Notice from Figure 2 that D2D ASE increases with increasing r_c due to reduced interference from active RRHs resulting from the effect of cooperatively scheduling, on the other hand in Figure 3, D2D ASE remains fairly constant with increasing r_c.

In Figure 4, the ASE is presented over varying D2D link distance threshold r_{th} when both ZFBF and NC-JCT is utilized, notice from the Figure that D2D ASE first increases and then decreases with increasing r_{th}, this is because more D2D links are activated when r_{th} is increased, however further increasing r_{th} means larger D2D link distance. It can be observed from the Figure 4 that at sufficiently large D2D link distance, the ASE increases and becomes fairly constant because all the users are on D2D transmission mode and no RRH is active. Besides, we can also see from Figure 4 that, D2D users

can accomplish improved ASE performance when ZFBF scheme is applied at the RRHs since the interference is diminished when the ZFBF is adopted, as analytically demonstrated in Section 3.

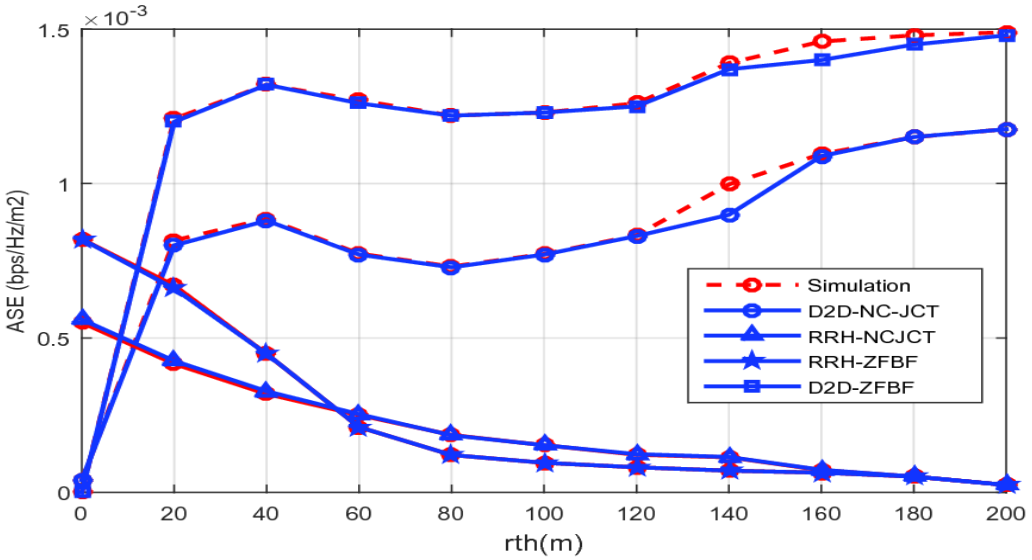

Figure 4. ASE with varying D2D link Threshold r_{th}

5 CONCLUSIONS

This paper studied the system capacity performance of D2D communication underlaying H-CRAN where two RRH cooperative transmission strategies are considered i.e., ZFBF and NC-JCT. It is observed that despite the benefit offered by RRH cooperation in improving the performance of some selected down link users, this gains actually comes at the cost of disabling other downlink users from being served on the same channels and thus leading to inefficient spectral resource utilization. To address this problem, D2D communication is utilize to serve as an alternative for users, which has shown to be effective in improving the spectrum utilization. Results from the analysis shows that the ASE decreases with increasing cluster size when either ZFBF or NC-JCT is adopted, because too many RRHs are selected to serve a small number of users thereby leading to wastage in the spectral resources. Meanwhile, activating D2D communications can offload the H-CRAN traffic and improve the ASE performance due to proximity gains. The results further demonstrate that the ASE of D2D users when ZFBF is employed outperforms that of the NC-JCT scheme.

REFERENCES

1. Cisco Systems Inc., Cisco Visual Networking Index*:* Global Mobile Data Traffic Forecast Update, 2014-2019. White Paper, Cisco, [Accessed on 12th February, 2017.] Available: http://www.cisco.com/c/en/us/solutions/collateral/service-provider/visualnetworking-index-vni/white paper c11-520862.html

2. Chen, S. and Zhao, J. (2014). The requirements, challenges, and technologies for 5G of terrestrial mobile telecommunication. IEEE Communication Magazine, vol. 52, pp. 36-43.

3. Peng, M., Li, Y., Jiang, J., Li, J. and Wang, C. (2014). Heterogeneous cloud radio access networks: A new perspective for enhancing spectral and energy efficiencies. *IEEE Transactions on Wireless Communication*, vol. 21, pp. 126-135.

4. Peng, M., Wang, C., Lau, V. and Poor, H.V. (2015). Fronthaul-constrained cloud radio access networks: Insights and challenges. *IEEE Transactions on Wireless Communication*, vol. 22, pp. 152-160.

5. Jonghyun, P., Euiseok, S. and Wonjin, S. (2009). Capacity analysis for distributed antenna systems using cooperative transmission schemes in fading channels. *IEEE Transactions on Wireless Communications*, vol. 8, pp. 586– 592.

6. Liu, Y.F., Dai, Y.H. and Luo, Z.Q. (2011). Coordinated Beamforming for MISO Interference Channel: Complexity Analysis and Efficient Algorithms. *IEEE Transactions on Signal Processing*, vol. 59, pp. 1142-1157.

7. Dahrouj, H. and Yu, W. (2010). Coordinated beamforming for the multi-cell multi-antenna wireless systems. *IEEE transactions on Wireless Communications*, vol. 9, pp. 1748-1759.

8. Tanbourgi, R., Singh, S., Andrews, J.G. and Jondral, F.K. (2014). A Tractable model for non-coherent joint transmission base station cooperation. *IEEE Transactions on Wireless Communications*, vol. 13, pp. 4959-4973.

9. Lee, N., David, M.J., Lozano, A. and Robert, W.H. (2015). Spectral efficiency of dynamic coordinated beamforming: A stochastic geometry approach. *IEEE Transactions on Wireless Communications*, vol. 14, pp. 230-241.

10. Asadi, A., Wang, Q. and Mancuso, V. (2014). A Survey on Device-to-Device Communication in Cellular Networks. *IEEE Communication Survey and Tutorials*, vol. 9, pp. 4959-4973.

11. Sun, H., Wildemeersch, M., Sheng, M. and Tony, Q.S.Q. (2015). D2D enhanced heterogeneous cellular networks with dynamic TDD. *IEEE Transaction on Wireless Communications*, vol. 14, pp. 4204-4218.

12. Liu, Z. Peng, T., Lu, Q. and Wang, W. (2012). Transmission capacity of D2D communication under heterogeneous networks with dual bands. Proceeding of the 7th International ICST Conference CROWNCOM, Stockholm, Sweden, June 2012.

13. Abana, M.A., Peng, M., Zhao, Z. and Olawoyin, L.A. (2016). Coverage and rate analysis in heterogeneous cloud radio access networks with device-to-device communication. *IEEE Access*, vol. 4, pp. 2357 – 2370.

14. Tanbourgi, R., Jakel, H. and Jondral, F. (2014). Cooperative interference cancellation using device-to-device communications. *IEEE Communication magazine*, vol. 52, pp. 118 - 124.

15. Mumtaz, S., Saidul Huq, K. and Rodriguez, J. (2014). Coordinated paradigm for D2D communications. Proc. *IEEE INFOCOM, Toronto, Canada*, pp. 718 - 723.

16. Li, J., Papadogiannis, A., Apelfrojd, R., Svensson, T. and Sternad, M. (2012). Performance evaluation of coordinated multipoint transmission schemes with predicted CSI. *IEEE 23rd International Symposium on Personal, Indoor and Mobile Radio Communications-(PIMRC), Sydney*, pp. 1055-1060.

17. Nigam, G. Minero, P. and Haenggi, M. (2014). Coordinated multipoint transmission in heterogeneous networks. *IEEE Transactions on Communications*, vol. 62, pp. 4134-4146.

18. 3rd Generation Partnership Project (3GPP), "Coordinated multipoint operation for LTE- advanced physical layer aspects", Sophia-Antipolis, France, Tech. Rep., TR 36.819 Sept 2011. Available online at http://www.qtc.jp/3GPP/Specs/36819-b10.pdf.